A real-time strain monitoring framework for UAV wings based on a dual-driven approach integrating physical models and data

Donglin Wu [1, a], Xuechen Liu [1, b], Ling Zhou [1, c, *]

[1] School of Aeronautics and Astronautics, Nanchang Hangkong University, Nanchang, 330063, China.

[a] lgnanming@163.com, [b] 1300756453@qq.com, [c, *] 70803@nchu.edu.cn

Abstract. With the increasing prevalence of drone applications, monitoring their health status has become crucial. This paper compares the prediction accuracy and spatial range of predictions between data-driven and dual-driven methods, which combine models and data. A real-time strain monitoring framework for UAV wings based on a dual-driven approach integrating physical models and data is proposed. This framework overcomes the limitations of single-method approaches and keeps prediction errors within 10%. Additionally, by utilizing real-time data from sensors and visualizing the predicted wing model, real-time monitoring of UAV wing strain is achieved. This provides a robust safeguard for the safe flight and mission execution of UAVs.

Keywords: UAVs; Dual-Driven Method; Prediction; Real-Time Monitoring; Multi-Fidelity Modeling.

1. Introduction

The significance of unmanned aerial vehicles (UAVs) in the modern aviation domain is increasing rapidly, with their applications expanding continuously in areas such as military reconnaissance [1], logistics transportation [2], and environmental monitoring [3]. The wings of UAVs, as a critical structural component, directly impact flight safety and mission execution effectiveness. Real-time monitoring of the state changes in physical models is an ongoing pursuit in engineering applications. It not only provides a more intuitive real-time reflection of the model's state but also enables operators to make timely adjustments based on the model's condition, thereby preventing potential failures or damages.

This paper proposes a real-time strain monitoring framework for UAV wings based on a dual-driven approach that integrates physics-based models and data. The objective is to overcome the limitations of single-method approaches, enhance monitoring accuracy, and expand the geometric range of predictions. Experimental validation demonstrates that the proposed algorithm performs well in terms of prediction accuracy and real-time capability, offering a novel technological means for UAV wing health monitoring.

2. Methods

2.1 Data Acquisition and Preprocessing

The data are derived from strain measurement experiments on UAV wing, utilizing high-precision strain gauge sensors installed on the wing surface to collect strain data in real-time. During flight, the wing structure of the UAV is primarily subjected to bending moments, shear forces, and torsional moments. For ease of calculation and to facilitate subsequent research, only the lift force acting on the wing is considered, and the wing loading is appropriately simplified to form a cantilever beam structural model [4,5].

A total of 18 strain gauges were installed on the wing, with 15 serving as test points and 3 as validation points. During the experiment, the wing was repeatedly loaded and unloaded, undergoing a total of 50 tests to avoid data randomness. The strain data collected after the wing stabilized were used as the measurement data. For the convenience of subsequent calculations, all strain data in this

paper are taken as positive values, since the negative sign only represents direction, not magnitude. Fig. 1 illustrates the installation locations of the strain gauges on the wing.

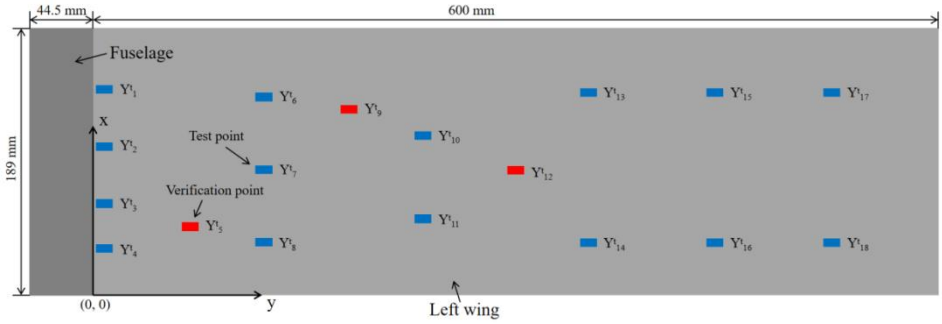

Fig. 1 Schematic Illustration of Strain Gauge Placement on the Wing

The collected data are normalized to scale the values within a unified range, facilitating subsequent model training and prediction. The wing projection is discretized in two dimensions. Within this two-dimensional space, the coordinates serve as the input to the model, while the strain values act as the response variables. The strain values from the 15 test points are utilized as feature variables and incorporated into this two-dimensional space.

2.2 Data-Driven Model

Bootstrap aggregating (Bagging) [6], also known as the bagging algorithm, is an ensemble learning method. Proposed by Leo Breiman in 1996, this algorithm constructs multiple sample sets by randomly drawing samples with replacement from the training set. Each training iteration generates a classifier that predicts the data. The final prediction result is determined through an aggregation strategy [7]. The flowchart of the algorithm is shown in Fig. 2.In this study, the Bagging algorithm is employed for strain prediction. The model training process for the regression problem is as follows: (1) Divide the dataset and construct an ensemble model using the Bagging algorithm. (2) Randomly draw multiple subsamples with replacement from the training dataset. (3) Train a decision tree model for each subsample. (4) Average the prediction results of all decision tree models to obtain the final prediction value, that is:

$$\Gamma = \frac{1}{m}\sum_{i=1}^{m} h_i(x) \tag{8}$$

where Γ is the final prediction result, m is the number of base models, $h_i(x)$ is the prediction result of the base model.

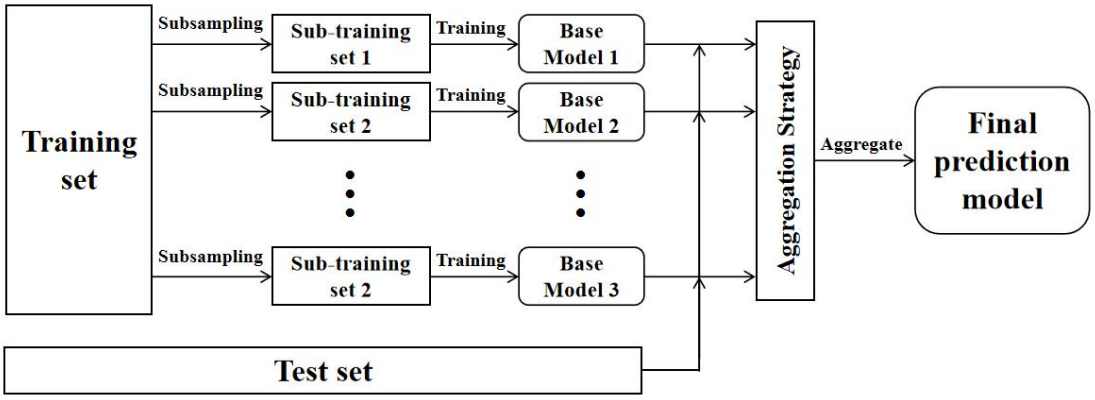

Fig. 2 Schematic Diagram of the Algorithm

The Bagging algorithm is employed to integrate multiple decision tree models. The three hyperparameters, namely the minimum number of samples per leaf node (MLS), the maximum number of splits in each decision tree (MNS), and the number of decision trees (NLC), are optimized using a random search approach. The optimal hyperparameters are identified by evaluating the coefficient of determination (R-Square, R2) of the models with randomly combined

hyperparameters. Additionally, cross-validation is utilized to assess the generalization ability of the model and to prevent overfitting. The values of the optimal hyperparameters are presented in Table 1.

Table 1. Values of the Optimal Hyperparameters.

MLS	MNS	NLC
2	17404	392

The 50 sets of strain data from the 15 measurement points are divided into training and test sets. The training set is used for model training, while the test set is used for model validation, with the Bagging algorithm employed for training. Compared to the entire two-dimensional space of the wing, the number of test points is smaller. Two models are considered: one is trained solely on the test points; the other first interpolates the entire wing's two-dimensional space based on the strain data from the 15 test points to obtain data for the entire wing surface, and then trains the model to derive the prediction model. Both models compare the predicted values at the test points after training with the average values of the test set to evaluate the model's accuracy. Fig. 3 shows the comparison between the results of the two training methods and the average values of the test set. Fig. 4 presents the relative errors of the predicted values before interpolation (Predicted Values Before Interpolation, PVBI) and the predicted values after interpolation (Predicted Values After Interpolation, PVAI).

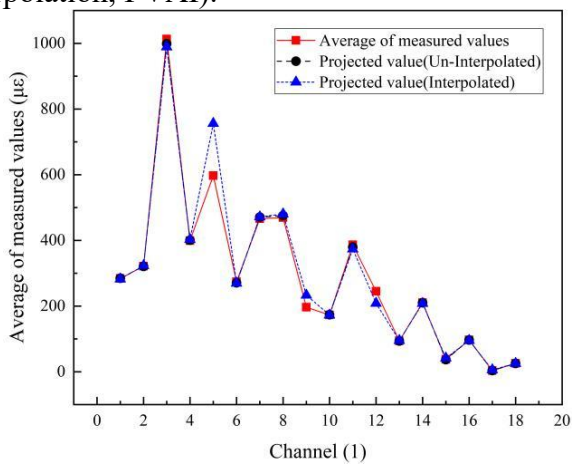

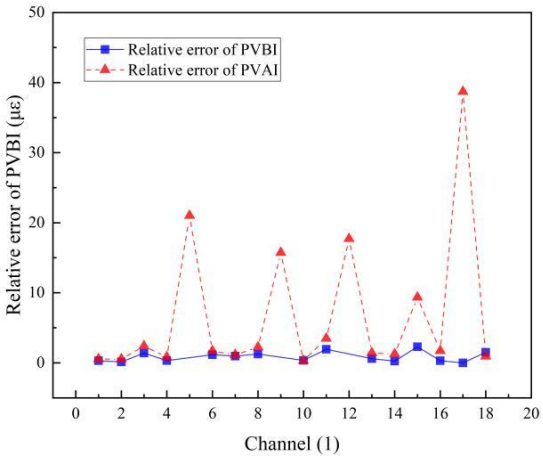

Fig. 3 Comparison of Different Training Results with the Average Value of the Test Set

Fig. 4 Relative Errors of Predicted Values Before and After Interpolation

The results indicate that the model trained solely on the test point data achieves higher prediction accuracy at the test points, with relative errors below 5%. However, this model is incapable of predicting the strain values at the validation points, as it is limited to the 15 test points. This falls short of the requirement for global prediction. The model trained after interpolation, although capable of global prediction, exhibits larger relative errors at certain points. Specifically, the maximum relative error occurs at channel 17, reaching 38%, while the relative errors at other channels are within 10%. Moreover, the relative errors at the three validation points are also substantial, ranging from 15% to 25%. Clearly, this model does not meet the global prediction requirement either. However, it is impractical to continuously increase the number of sensors. Therefore, it is necessary to combine simulation data for prediction and employ a dual-driven approach that integrates data and models for prediction.

2.3 Dual-Driven Approach with Data and Physics-Based Models

Numerical simulations of the wing tests were conducted using simulation software, with boundary conditions and loads identical to those in the tests. The material model was derived from previous studies. The simulation results were indexed based on the two-dimensional coordinates of the wing, and combined with the measured data to form the original dataset.

The original dataset was divided into training and test sets at a ratio of 4:1. The training set was used to train the prediction model using the Bagging algorithm. The predicted values at the 18

channels and the average values of the test set are shown in Fig. 5. The relative errors of the predicted values are presented in Fig. 6.

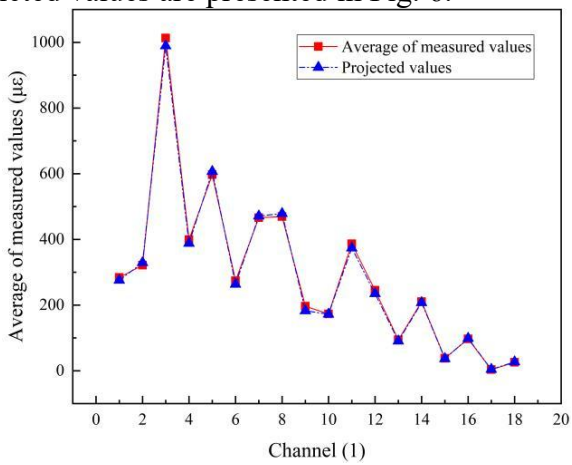

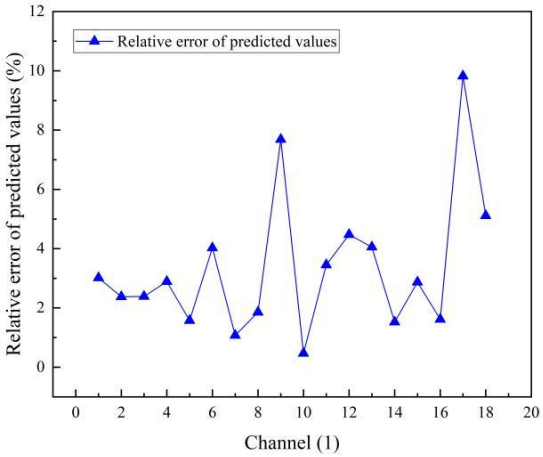

Fig. 5 Predicted Results and the Average Values of the Test Set

Fig. 6 Relative Errors of Predicted Values

As shown in the figures, the predicted values from the model are in close agreement with the measured values. The prediction performance at the three validation points (channels 5, 9, and 12) is also satisfactory, with relative errors all within 10%, meeting the required prediction accuracy. At channel 17, the relative error reaches 9.82%. This is due to the small magnitude of the measured value itself; even a slight deviation between the predicted and measured values can cause a significant fluctuation in the relative error. However, the prediction accuracy requirement is still met.

3. Visualization results

3.1 Establishment of the Model Library

Given that the wing employs a linear loading method, the working condition can be simplified to a linear loading ranging from 0 to 1. The strain variation curve during testing is shown in Fig. 7, where (a) represents the strain curve variation during the loading process, and (b) shows the strain variation after ignoring the time factor. The predicted model is used as the final strain state, with the initial strain state set to 0. Linear interpolation is performed from 0 to 1, generating a total of 100 models, which form the prediction model library corresponding to the strain states under different loads. Fig. 8 presents the strain contour maps of several interpolated prediction models.

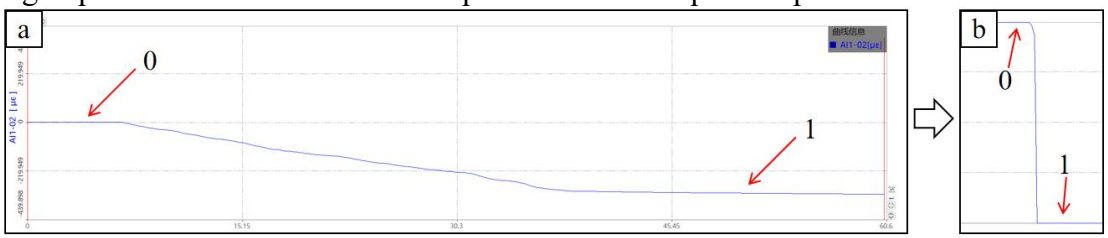

Fig. 7 Strain Variation Curve of the Wing During Testing. (a). Strain Curve Variation During the Loading Process (b). Strain Variation After Ignoring the Time Factor

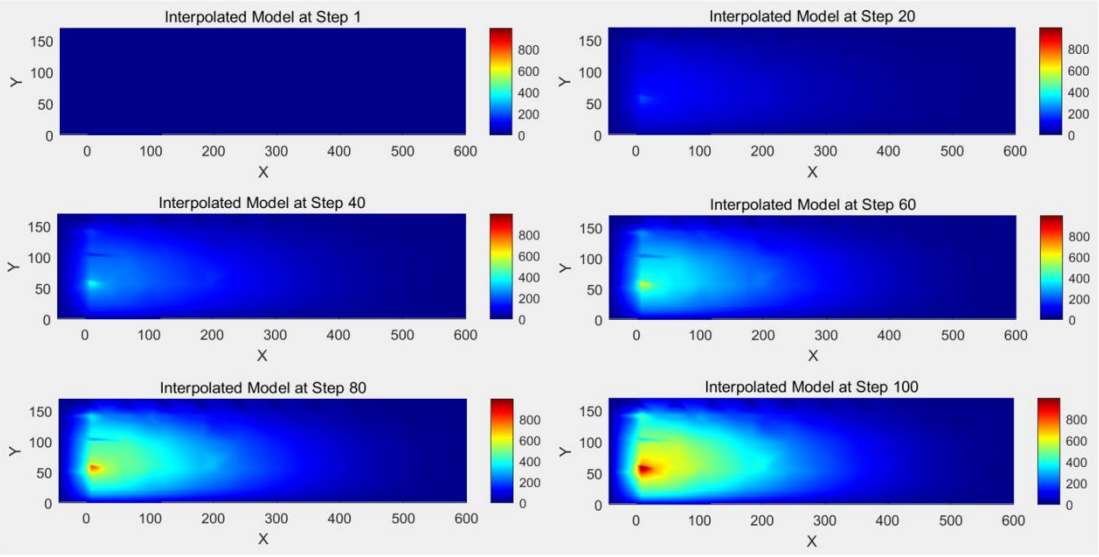

Fig. 8 Strain Contour Maps of Selected Interpolated Prediction Models

3.2 Real-Time Monitoring of Wing Strain

The strain data collected by the strain acquisition instrument enables the prediction model to respond promptly and update the strain contour maps in real-time. The specific implementation process is as follows:

Firstly, by inputting the spatial coordinates (x,y) of the corresponding measurement points, and combining the grid data of the model, the minimum distance between the input coordinate points and the grid points is calculated, thereby locating the nearest grid point.

Secondly, for each strain value collected, all interpolated models are traversed to calculate the strain value at the collection point within each model, and then compared with the input strain value. The MSE is employed as the evaluation criterion, aiming to select the model with the smallest error relative to the input strain value. Multiple collection point data can be integrated for a comprehensive assessment. Through this approach, the best-matching model can be effectively identified.

Subsequently, to ensure real-time visualization of the results, a method of dynamically updating the graphics is employed. Each time the best-matching model is identified, the system clears the current display on the graphical interface and redraws the new strain contour map.

Lastly, a warning mechanism is incorporated. If the input strain value exceeds the safety threshold (for example, set at 1200με), indicating that the load on the wing is too high, the warning mechanism is triggered. The system alerts the user to the potential risk of wing damage through audio and pop-up notifications.

Based on the real-time collected data and this algorithmic model, real-time monitoring of wing strain can be achieved, and potential damages can be adjusted in a timely manner. Fig. 9 shows the strain contour maps corresponding to some continuously collected real-time data.

The advantage of this method lies in its ability to automatically select the most suitable interpolation model, reducing the need for manual intervention. Moreover, by dynamically updating the contour maps and providing real-time feedback, it offers intuitive and efficient decision support for operators.

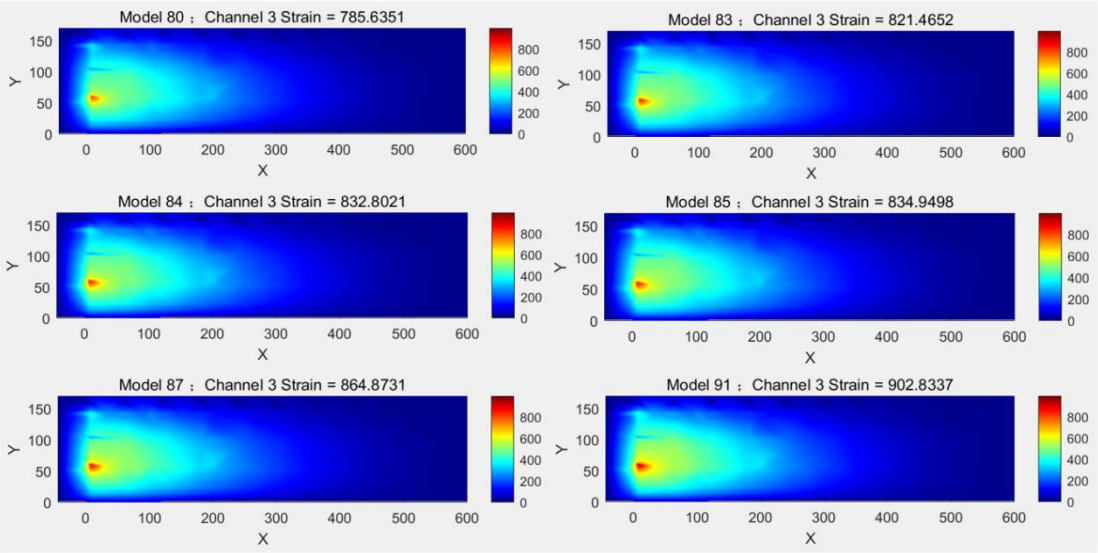

Fig. 9 Strain Contour Map Corresponding to Real-time Collected Continuous Data

3.3 Verification of Prediction Results

To verify the prediction results of the model under different states of the wing, this paper integrates the data from channels 3, 5, and 8 to determine the best prediction model through a comprehensive evaluation based on the value of MSE(Mean-Square Error, MSE). Let the predicted value be PV, the test value be TV, and the relative error be RE. The subsequent numbers indicate the group, meaning that three validations were conducted. The data are shown in Table 2.

Table 2. Comparison of Prediction and Test Results

Channel	PV-1 (με)	TV-1 (με)	RE-1 (%)	PV-2 (με)	TV-2 (με)	RE-2 (%)	PV-3 (με)	TV-3 (με)	RE-3 (%)
1	114.19	113.66	0.47	169.89	173.95	2.33	225.59	224.32	0.57
2	136.21	151.14	9.88	202.65	212.45	4.61	269.10	264.83	1.61
3	410.02	407.25	0.68	610.03	610.81	0.13	810.04	811.93	0.23
4	160.71	176.07	8.73	239.11	265.59	9.97	317.51	331.62	4.25
5	251.23	249.05	0.87	373.78	374.95	0.31	496.33	487.29	1.85
6	109.07	109.66	0.54	162.28	169.67	4.36	215.48	219.97	2.04
7	195.24	202.51	3.59	290.48	296.17	1.92	385.73	385.99	0.07
8	198.18	205.48	3.56	294.86	302.21	2.43	391.53	393.10	0.39
9	75.54	80.03	5.61	112.39	123.27	8.82	149.24	158.67	6.01
10	71.34	70.28	1.51	106.15	110.84	4.23	140.95	138.14	2.03
11	154.69	156.44	1.12	230.15	238.03	3.31	305.61	304.25	0.45
12	97.14	98.67	1.55	144.53	148.54	2.70	191.92	196.79	2.47
13	37.41	35.15	6.43	55.66	56.52	1.52	73.91	74.68	1.03
14	85.92	82.48	4.17	127.84	130.10	1.74	169.75	172.56	1.63
15	15.20	14.58	4.25	22.61	22.84	1.01	30.02	29.15	2.98
16	40.82	37.86	7.82	60.74	56.89	6.77	80.65	76.44	5.51
17	1.71	1.56	9.04	2.54	2.32	9.48	3.37	3.07	9.77
18	11.15	10.21	9.21	16.59	15.16	9.43	22.03	20.15	9.33

As shown in the table, the relative errors for all groups are within 10%, indicating that the prediction model achieves a high level of accuracy and meets the prediction requirements.

4. Conclusion

This paper proposes a real-time strain monitoring framework for UAV wings based on a dual-driven approach that integrates physics-based models and data. Through experimental validation, the algorithm demonstrates excellent performance in terms of prediction accuracy and real-time capability, offering a new technological means for the health monitoring of UAV wings.

The application of this algorithm not only enhances the accuracy and reliability of UAV wing strain monitoring but also provides a robust safeguard for the safe flight and mission execution of UAVs.

References

[1] Lee M, Choi M, Yang T, et al. A Study on the Advancement of Intelligent Military Drones: Focusing on Reconnaissance Operations[J]. IEEE Access, 2024, 12: 55964-55975.

[2] Cui H, Li K, Jia S, et al. Dynamic collaborative truck-drone delivery with en-route synchronization and random requests[J]. Transportation Research Part E: Logistics and Transportation Review, 2024, 192: 103802.

[3] Bakirci M. Smart city air quality management through leveraging drones for precision monitoring[J]. Sustainable Cities and Society, 2024, 106: 105390.

[4] Yan C, Zhang S, Zhuo N, et al. MECHANICAL MODEL AND DATA PROCESSING OF LOAD MEASUREMENT TEST FOR THE AIRPLANE'S WING STRUCTURE[J]. Acta Aeronautica et Astronautica Sinica, 2000, 21(1): 56-59.

[5] Jiang B, Liu G. Structural Mechanics[M]. BeiJing: National Defense Industry Press, 1980.

[6] Breiman L. Bagging predictors[J]. Machine Learning, 1996, 24(2): 123-140.

[7] Shen Y, Shao Y, Zong P, et al. A Precise and Effective Multi-Base Model Framework for Book Classification Based on Bagging[J]. Information Technology, 2024(9): 20-28.